Bioorganic & Medicinal Chemistry 18 (2010) 3261–3269

Contents lists available at ScienceDirect

Bioorganic & Medicinal Chemistry

journal homepage: www.elsevier.com/locate/bmc

3′-(1,2,3-Triazol-1-yl)-3′-deoxythymidine analogs as substrates for human and *Ureaplasma parvum* thymidine kinase for structure–activity investigations

Jay Lin [a,†], Vincent Roy [b,†], Liya Wang [a], Li You [b], Luigi A. Agrofoglio [b,*], Dominique Deville-Bonne [c], Tamara R. McBrayer [d,e], Steven J. Coats [e], Raymond F. Schinazi [d], Staffan Eriksson [a,*]

[a] Dpt. Anatomy, Physiology and Biochemistry, Veterinary Medical Biochemistry, Swedish University Agricultural Sciences, Uppsala, Sweden
[b] Institut de Chimie Organique et Analytique, CNRS UMR 6005, Université d'Orléans, 45067 Orléans Cedex 2, France
[c] Laboratoire d' Enzymologie Moléculaire et Fonctionnelle, Université Pierre et Marie Curie, Paris, France
[d] Center for AIDS Research, Lab. Biochem. Pharmacol., Dpt. Pediatrics, Emory University School of Medicine and Veterans Affairs Medical Center, Decatur, GA 30033, USA
[e] RFS Pharma, LLC, 1860 Montreal Road, Tucker, GA 30084, USA

ARTICLE INFO

Article history:
Received 12 November 2009
Revised 4 March 2010
Accepted 11 March 2010
Available online 15 March 2010

Keywords:
Thymidine kinase
Mycoplasma
Nucleoside analogs
Microwave
Click-chemistry
Structure function-relationship
AZT
Ureaplasma parvum
Huisgen reaction

ABSTRACT

The pathogenic mycoplasma *Ureaplasma parvum* (*Up*) causes opportunistic infections and relies on salvage of nucleosides for DNA synthesis and *Up* thymidine kinase (*Up*TK) provides the necessary thymidine nucleotides. The anti-HIV compound 3′-azido-3′-deoxythymidine (AZT) is a good substrate for TK. Methods for a rapid and efficient synthesis of new 3′-α-[1,2,3]triazol-3′-deoxythymidine analogs from AZT under Huisgen conditions are described. Thirteen 3′-analogues were tested with human cytosolic thymidine kinase (hTK1) and *Up*TK. The new analogs showed higher efficiencies (K_m/V_{max} values) in all cases with *Up*TK than with hTK1. Still, hTK1 was preferentially inhibited by 9 out of 10 tested analogs. Structural models of *Up*TK and hTK1 were constructed and used to explain the kinetic results. Two different binding modes of the nucleosides within the active sites of both enzymes were suggested with one predominating in the bacterial enzyme and the other in hTK1. These results will aid future development of anti-mycoplasma nucleosides.

1. Introduction

2′-Deoxynucleoside kinases (dNKs) such as thymidine kinases 1 (TK1) are found in most organisms including viruses, bacteria and mammals. TK primarily activates thymidine (dThd) and 2′-deoxyuridine (dUrd) by phosphorylation of the 5′-OH group, forming a charged nucleotide, which is trapped in the cell. The nucleoside monophosphates formed, will after further phosphorylation steps be incorporated into by DNA polymerases.[1–3] The first phosphorylation reaction is often rate limiting and TK1 expression is closely associated with cell proliferation, with a peak in the S-phase of mammalian cells (for TK1) followed by degradation during mitosis.[2,4,5] High TK1 levels are found in malignant cells and TK1 has been used as a tumor marker in cancer diagnostics.[6]

Nucleoside analogs, mimicking the building blocks of DNA, utilize dNKs as activating enzymes in case of several anticancer and antiviral prodrugs[3–5] such as 3′-azido-3′-deoxythymidine (AZT) used in HIV treatment. Its triphosphate form blocks viral reverse transcriptase and results in discontinued virus replication.[7] AZT also inhibits the growth of gram negative bacteria like *Escherichia coli*.[8,9]

The hTK1 family together with the other dNK families are key enzymes in the salvage pathway, whereas de novo nucleotide synthesis requires ribonucleotide reduction as well as other enzymatic reactions.[3,5] Not all organisms have the de novo pathway and the mycoplasma *Ureaplasma parvum* (*Up*), previously called *Ureaplasma urealyticum*, is an example of an organism lacking this pathway and therefore relies entirely on the salvage pathway.[10–12] *Up* is a free-living self-replicating bacteria containing one of the

Abbreviations: ATP, adenosine triphosphate; AZT, 3′-azido-thymidine; BSA, bovine serum albumin; dAK, deoxyadenosine kinase; CuAAC, copper (I) catalyzed azide-alkyne cycloaddition; DMSO, dimethyl sulfoxide; dThd, thymidine; DTT, dithiothreital; dUrd, deoxyuridine; hTK1, human thymidine kinase 1; dThd, thymidine; *Up*, *Ureaplasma parvum*; *Up*TK, *Ureaplasma parvum* thymidine kinase; Vv, Vaccinia virus; TLC, thin layer chromatography; NMR, nuclear magnetic resonance; HRMS, high resolution mass spectrometry; HPLC, high-performance liquid chromatography; pdb, protein database file; IC_{50}, median inhibitory concentration.

* Corresponding authors. Tel.: +33 2 3849 4582; fax: +33 2 3851 0728 (L.A.A.); tel.: +46 7099 08059 (S.E.).
E-mail addresses: luigi.agrofoglio@univ-orleans.fr (L.A. Agrofoglio), staffan.eriksson@afb.slu.se (S. Eriksson).
† These authors equally contributed to this work.

0968-0896/$ - see front matter © 2010 Elsevier Ltd. All rights reserved.
doi:10.1016/j.bmc.2010.03.023

smallest genomes known to date.[10,12–14] and is found in up to 80% of all adults.[12–14] *Up* colonizes the urogenital tract and has the ability to harvest ATP from urea.[10,13,14] *Up* is associated with pregnancy complications such as infertility, altered sperm motility and pneumonia in the neonate. This type of infection could result in chronic lung disease with severe scaring on lung tissue causing an increased mortality.[14,15] The range of potential antibiotics against *Up* is limited because of the absence of a cell wall and limited biosynthetic pathways compared to other organisms.[10–12,16] In *Mycoplasma/Ureaplasma* two dNKs are present, a TK and a dAK,[10,11,13,16] making these important medicinal target enzymes, since these salvage enzymes are essential for DNA precursor synthesis and their inhibition would stop bacterial growth. *Up*-TK has previously been crystallized and characterized as strictly pyrimidine specific.[11] Some nucleoside analogs were evaluated as potential inhibitors of *Up*TK.[11,17] Human TK1 has also been crystallized in parallel to *Up*-TK revealing a similar 3D structure,[17–19] despite the relatively low amino acid similarity (30%). Some differences in the specificities of *Up*-TK and hTK1 were detected, particularly with substitutions at the 5- or 3-position of the base and 3′-position of the sugar.[11,17]

AZT is well accepted as substrate by the TK1 family[11,20] and triazol-derivates have been studied intensively for many years due to their high reactivity, ease of preparation, anti-microbial, antiviral, anti-inflammatory and anti-tumor properties.[21–27] Some inactive and nontoxic 3′(1,2,3-triazol-1-yl)-3′-deoxythymidines[28] were already synthesized but their phosphorylation mechanisms have not been studied.

Here we describe the synthesis and an enzymatic characterization of new 3′-substituted thymidine analogues, starting from AZT forming [1,2,3]-triazoles via copper(I) catalysed reactions. Pharmacomodulation has become central to drug discovery and has played a major role in the search for new treatments of viral diseases. However, the discovery and process optimization of potential agents is often slow, expensive and involves complex synthetic schemes. The 'click chemistry' proposed by Sharpless et al.[29] has emerged as a fast and efficient approach to simplify compound synthesis. The Huisgen 1,3-dipolar cycloaddition of azides and terminal alkynes is one of the best known and powerful click reactions,[30] which is compatible with microwave activation and can offer a rapid method to aid in the drug discovery process.[31]

Structural models of *Up*TK and hTK1 in complex with several of the new analogues based on the crystal structures of both enzymes[18,19] were built and used in this study to explain the differences in substrate selectivity and catalytic rates. The result increase our understanding of the mechanisms of TK enzymes and may help in future design of selective and efficient anti-*Up* agents. Antibiotic resistance in pathogenic bacteria has become a major public-health risk, therefore alternative antibiotics with new modes of action are needed and nucleoside analogues have the potential to be one of these new antibiotics.[17,32,33]

2. Results and discussion

2.1. Results

Compounds containing a [1,2,3]-triazole moiety are often associated with interesting biological activities, such as anti-microbial, antiviral and anti-proliferative effects. Since the discovery of copper(I) as catalyst of Huisgen's 1,3-dipolar cycloadditions, this reaction has been shown to be highly specific, irreversible, regioselective and chemo-selective.[29b] Here we report the synthesis of a several AZT analogues bearing a 1,2,3-triazole moiety at 3′-position under microwave-assisted CuAAC.[34] Microwave heating is known as a powerful technique to promote a variety of chemical reactions,[35] including some alkyne-azide cycloadditions, with substantial decreases in reaction times. The 1,3-dipolar cycloaddition reaction was conducted with microwave activation in a water/*tert*-butanol (1:1) solvent mixture at 125 °C catalyzed by Cu(0)/$CuSO_4$[36] and at room temperature for compounds **7**, **10** and **11**, catalyzed by sodium ascorbate/$CuSO_4$[37] (Fig. 1).

Both methods generate the in situ Cu(I) catalyst to form the desired compounds with a complete conversion of starting materiel, in a fully regioselective (1,4) manner, without contamination by the 1,5-regioisomer. To provide a starting point for a detailed structure–activity study, diverse alkyne substituents, such as alcohol, alkyl, aromatic, and halogen derivatives, were utilized. The reactions were monitored by TLC.

All compounds **1**–**13** (Fig. 2) were isolated in high yields, ranging from 81% to 96%. Complete consumption of AZT occurred under microwave irradiation in 2–120 min reactions, depending on the substituents, and was followed by 12 h at room temperature. The regioselectivity of the ligation leading to 1,4-disubstitued-[1,2,3]-triazole moiety was confirmed by NMR using ^{1}H, ^{13}C long range correlation spectra (HMBC). It is interesting to note that the reaction leading to compound **1**, which has been previously reported to need 10 h,[28c] occurred under our optimized conditions within 10 min. Compounds **1**, **9**, **12** and **13** have already been reported to be devoid of significant antiviral activity.[28] They were included in our study to investigate the structure–activity relationship with the key bacterial enzyme *Up*TK.

2.1.1. In vitro activity of the 3́-substituted analogs with hTK1 and *Up*TK

The phosphorylation of different nucleoside analog by *Up*-TK and hTK1 is reported in Table 1. The activity with 100 μM ATP and dThd was set to 100%. All compounds **1**–**13** are similarly phosphorylated by hTK1 at 100 M, (Table 1).

The efficiency of phosphorylation was in general about two times higher with *Up*TK compared to hTK1 and particularly for **6** and **8**, **10**–**13** (Tables 1 and S1). More specifically, **13** was five times more potent with *Up*TK than hTK1. Compared to dThd, AZT showed 28% relative activity with *Up*TK and 47% with hTK1, as previously reported.[17] Enzyme kinetic studies with hTK1 and *Up*TK were done using [γ-^{32}P]-ATP transfer assay with varying concentrations of nucleosides. The kinetic results (Table S1) appeared to follow Michaelis Menten kinetics (Fig. S1) and the natural substrate dThd showed as expected the lowest K_m and highest V_{max} values with both enzymes.

AZT was a relatively good substrate for both enzymes (50% compared to dThd). Compounds **4**–**13** were in all cases more efficiently phosphorylated with *Up*TK than with hTK1. While compound **6** showed the overall lowest K_m values with *Up*TK, the largest relative difference was found with **11**, 10-times higher with *Up*TK than hTK1 (Fig. 3 and Table S1).

However, the overall relative efficiency was low and in the best cases it reached about 1% of dThd (set to 100%). Compound **6**

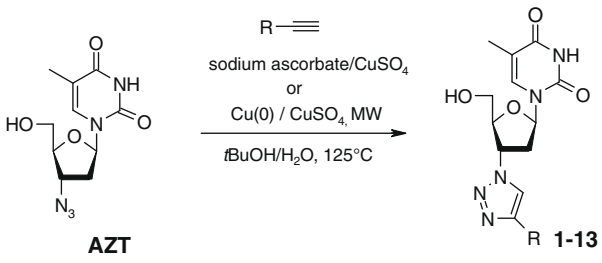

Figure 1. A scheme summarizing the synthesis of AZT derived triazoles via a CuAAC.

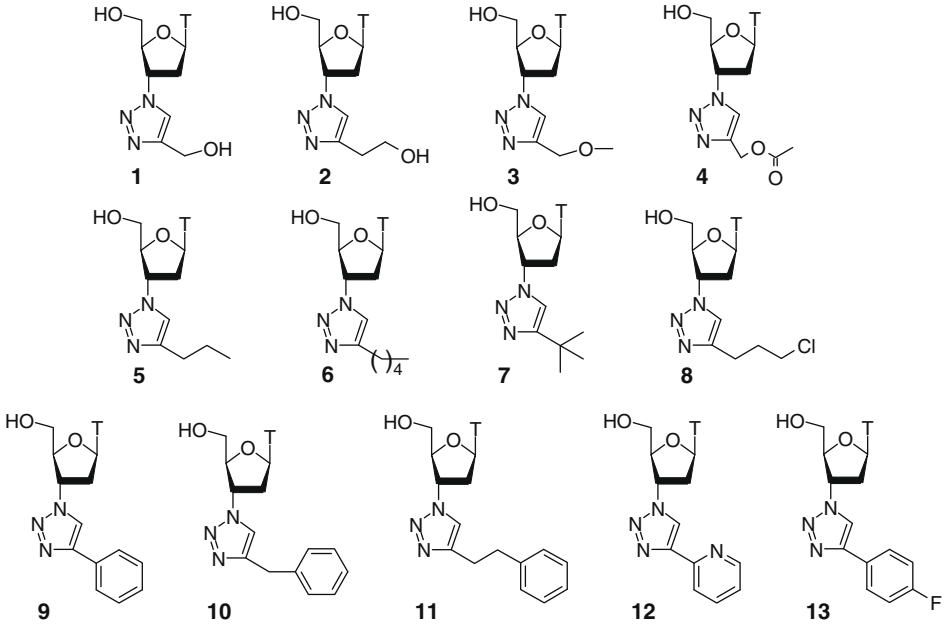

Figure 2. Synthesized compounds.

Table 1
Nucleoside analog phosphorylation by *Up*TK and hTK1. The activity with 100 M ATP and nucleosides, respectively, are presented with dThd activity set to 100%

Compounds	Relative activity (%)	
	*Up*TK	hTK1
dThd	100	100
AZT	27.8 ± 1.2	47.3 ± 0.4
1	Nd[a]	Nd[a]
2	4.1 ± 0.2	2.2 ± 0.1
3	1.6 ± 0.2	1.3 ± 0.01
4	3.9 ± 0.2	2.4 ± 0.1
5	6.5 ± 0.1	2.7 ± 0.2
6	7.2 ± 0.9	1.9 ± 0.04
7	4.7 ± 0.7	2.2 ± 0.1
8	8.7 ± 1.1	2.9 ± 0.1
9	5.5 ± 0.5	2.1 ± 0.1
10	11.6 ± 1.2	4.8 ± 0.1
11	12.3 ± 1.8	2.4 ± 0.1
12	7.1 ± 1.2	3.1 ± 0.04
13	13.7 ± 1.1	2.6 ± 0.2

The relative activity values are means ± SEM of three independent determinations. The specific activities of *Up*TK and hTK1 are 1140 and 757 nmol dTMP/min per mg, respectively.

[a] Nd: Not determined.

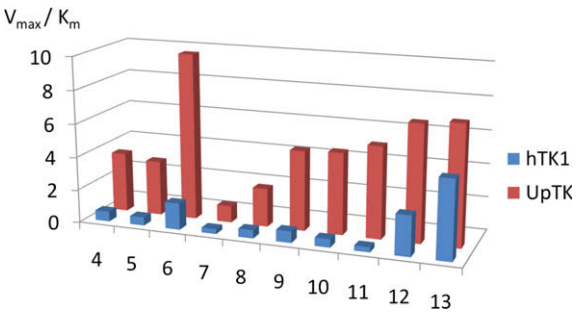

Figure 3. Catalytic efficiency phosphorylation of compound **4**–**13** by hTK1 and UpTK.

showed 1.6% relative efficiency with *Up*TK and was the best phosphorylated bulky 3′-substitution, followed by **12**–**13**. Compounds **9**, **12**–**13**, consisting of various phenyl-analogues had much higher K_m values (30–40 M) compared with the other compounds. The V_{max} values of *Up*TK for these compounds were 3–4 times lower than with AZT and the K_m values with hTK1 were in general higher than *Up*TK except in case of **13**, containing a phenyl-fluorine moiety. The K_m values for **13** were 10 M and 29 μM with hTK1 and *Up*TK, respectively.

2.1.2. Inhibition studies with the 3′-dThd substituted analogs

The IC_{50}-values of AZT and compounds **4**–**13** for hTK1 and *Up*TK were determined (Table 2).

In case of **12** and **13**, the lowest IC_{50}-values were 40–50 M with hTK1 and 71 M and 211 M with *Up*TK, respectively. The largest differences in IC_{50}-values between on both enzymes were found with **4** (fivefold), **12** (fourfold) and **7** (threefold); in all cases, the lower IC_{50}-values were observed with hTK1. Adding an extra spacer between the triazole and phenyl moiety lowered the IC_{50}-value by almost threefold (from **9** to **10**) in case of *Up*TK but also to some extent with hTK1. By extending the spacer without the phenyl moiety (**5**–**6** and **8**), no major changes with *Up*TK were found, while with hTK1 the IC_{50}-values decreased 4–3-fold in case of **8** and **5** compared to **6**. Taken together, these results reveal that most of the analogues **4**–**13** were better inhibitors of hTK1 compared to

Table 2
The IC_{50}-values (means and SEM from three determinations) were determined with 1 μM ^{3}H-dThd and additions of nucleoside analogues (20–500 μM)

Compounds	IC_{50} (μM)	
	*Up*TK	hTK1
AZT 4	12.5 ± 9.2	3.0 ± 3.7
5	208 ± 32	105 ± 23
6	189 ± 44	311 ± 37
7	318 ± 59	114 ± 53
8	150 ± 25	86 ± 31
9	200 ± 3	99 ± 2
10	73 ± 19	78 ± 36
11	120 ± 31	60 ± 23
12	211 ± 21	53 ± 23
13	71 ± 13	44 ± 10

*Up*TK. However, compound **13** was unique because it was the best inhibitor and one of the best substrate for both enzymes.

2.1.3. Model construction of nucleoside analogs in TK1 active site

Multiple sequence alignment of human, *Vaccinia virus (Vv)* and several bacterial TK sequences are shown in Figure 4. The sequence identity was about 29% between hTK1 and *Up*TK. Phylogenetic analyses[32,33,39] suggested that hTK1 is in the same subgroup as TKs of gram positive bacteria, while gram negative bacteria form another group with regard to the P-loop and Mg^{2+} binding-motif sequences. The amino acid composition of the P-β hairpin differs between the TKs, e.g., a serine rich region at position 62–64 was observed in hTK1, whereas only Ser54 is found in *Up*TK (Fig. 4).

The lasso loop is another important secondary structure element with high sequence diversity, containing inserts and short deletions. Bacterial TKs have more extended loops in this region than hTK1 and *Vv*TK (Fig. 4). Gram negative bacteria contain a conserved Gln169 (using the *E. coli* numbering), which probably form main chain hydrogen bonds with the N3 position of the nucleoside base just like Ile178 in *Up*TK.[17] The *E. coli* TK also has a conserved hydrophobic Val171 which probable interact with the 2-oxygen position of the base, like the corresponding Lys 180 in *Up*TK.[17] These features were less clear in the gram positive bacteria-hTK1-*Vv* group, but at least the corresponding residues were hydrophobic (Fig. 4). In hTK1, Gly176 is responsible for a hydrogen bond with the 3́-oxygen of the sugar. Glu98 is the catalytic base assisting in the phosphoryl transfer from ATP to 5́-OH and this residue is conserved in all organisms. *Up*TK is the only TK having a cysteine, Cys183 in the lasso loop (Fig. 4 and S3), and this may be used as a target in anti-*Up*TK agent development. Differences in the TK structures were observed when hTK1-dTTP and *Up*TK-dTTP complexes were compared and superimposed with PyMOL (Fig. 5A). The longer *Up*TK lasso loop section seen in the sequence alignment (Fig. 4), extended the hTK1 lasso loop starting from Lys166 to Asp176 (Fig. 5A).

Analogue **13** which had the lowest IC_{50}-values with both enzymes was modelled into the active sites of the hTK1 (1W4R) and *Up*TK (2UZ3) structures. These TK structures were chosen because they had visible lasso loops and P-hairpins. The base and sugar position of **13** fitted well with the available crystal structures of hTK1/*Up*TK in complex with dTTP[17–19] (Fig. 5B and C and S3). All the relevant enzyme–residues interactions were almost preserved (indicated by triangles in Fig. 4).

Conformation A was found with **13** modelled into the active site of *Up*TK. The 3́ triazole-ring adopted a conformation (A) where it interacted with Gly182 and thus it was in a bent positioned between the lasso loop and P-hairpin (Fig. 5C and S3B). In conforma-

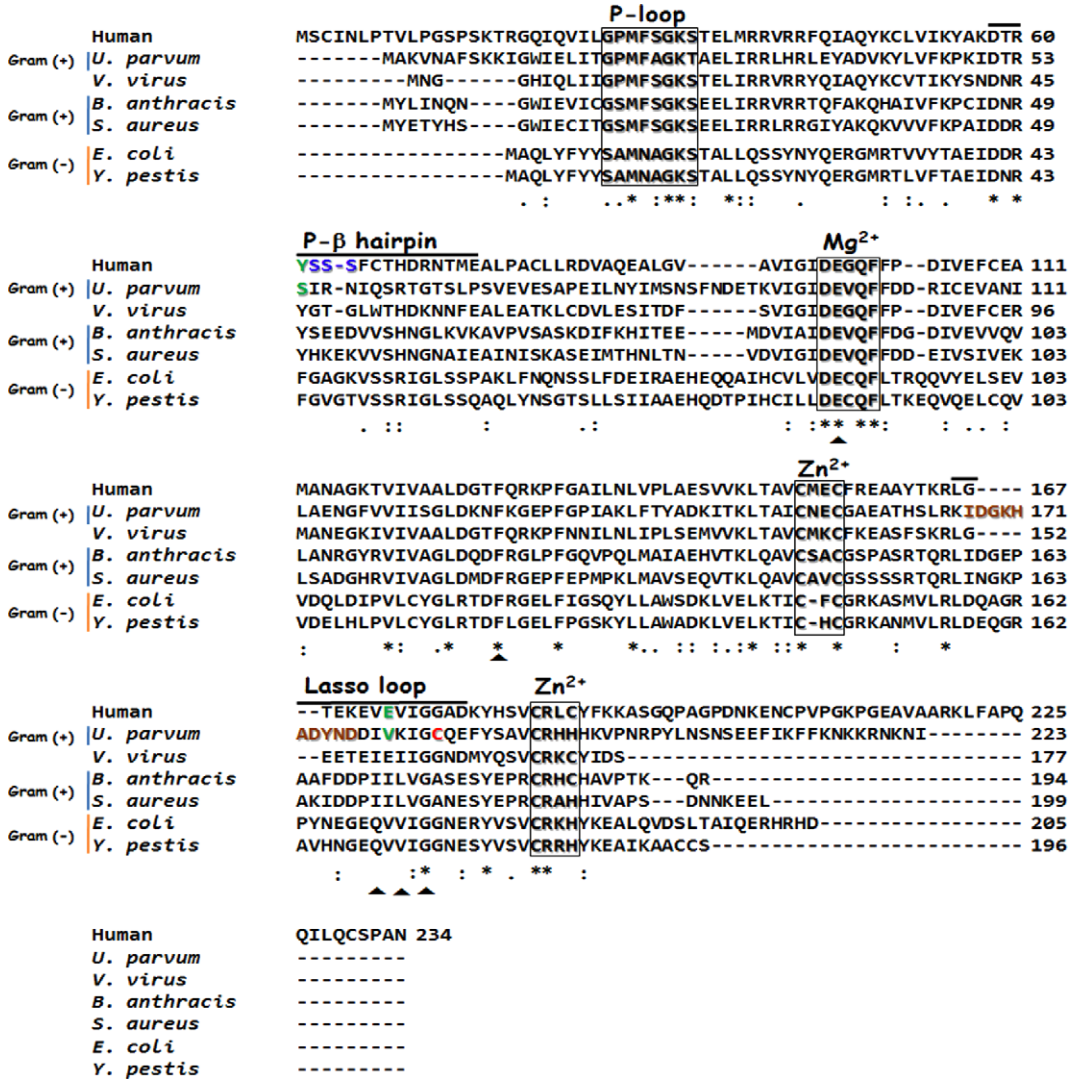

Figure 4. Comparison of amino acid sequence alignment of human, Vaccinia virus *(Vv)* and several bacterial TK.

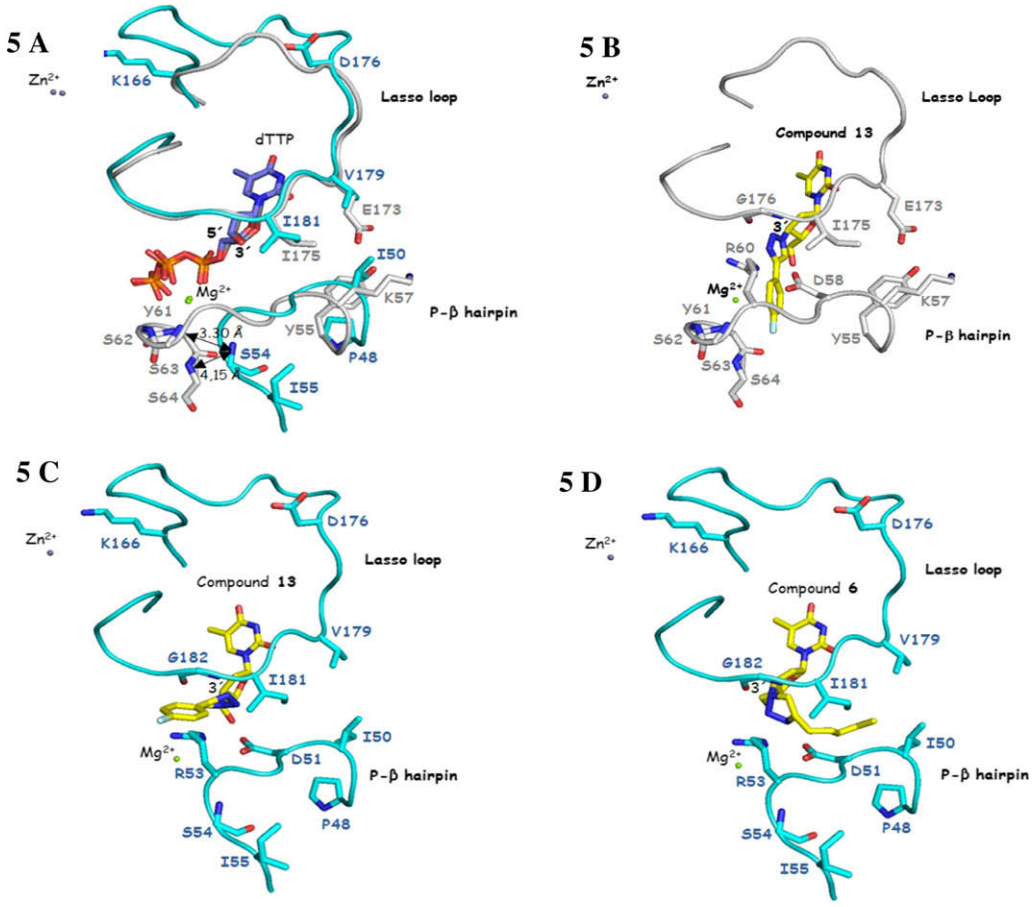

Figure 5. dTTP, compound **6** and **13** docked in the active site of HTK1 (grey) and *Up*TK (turquoise).

tion A, the cyclic triazole-phenyl moiety is positioned between the hydrophobic backbone of Gly182 and side chain of Arg53, however it is also partly exposed to solvent and there were no interactions with the other active site residues (Fig. 5C and S3B). Modelling **13** into the hTK1 structure produced another conformation (B) and in this case the 3́-triazole-phenyl moiety was instead shifted 90°, going straight through the P-hairpin and retained interactions with Gly182. Here the triazole phenyl-fluorine atom may form a main chain hydrogen bond with either Ser63 or Ser64 (Fig. 5B ant S3D) and apparently Tyr61 makes this possible by extending the hairpin. The corresponding *Up*TK Ser54 is positioned 3.30 Å or 4.15 Å from hTK1 Ser63 or 64, respectively (Fig. 5A and S4), and seems also available for this interaction. However, the *Up*TK Arg53 side chain might prevent this, because of a clash with the triazole phenyl moiety (Fig. S4A). This may explain the hTK1 preference for conformation B rather than A, and the low K_m-value for **13**.

Modelling compound **6** in the active site of *Up*TK revealed that the long 3́ hydrophobic triazole pentyl carbon substitution was located along the cleft between lasso loop and P-β hairpin. The shorter side chain of Val179 of the lasso loop and different located Pro48, in comparison with corresponding hTK1 amino acids (Glu173 and Tyr55) makes the cleft more hydrophobic and larger in *Up*TK (Fig. 5A and C and S5). This might explain the higher relative efficiency for compound **6** in *Up*TK than hTK1.

3. Discussion

The copper(I) azide-alkyne 1,3-dipolar cycloaddition of AZT gave easy access to a small library of compounds. The Huisgen cycloaddition reaction was performed under microwave irradiation in one step, starting from unprotected AZT. Some 1,2,3-triazole AZT analogues have previously been synthesized, and were found to lack significant activity against a set of viruses (HIV, Vaccinia virus, Cowpox virus, etc.).[28] The lack of activity of these analogues may be due to a failure to be phosphorylated by the necessary cellular or viral kinases. That is why in this study, a variety of different chemical structures have been attached to the 3′-position of AZT, to gain a better understanding of the structure–activity relationship of hTK1 and *Up*TK.

U. parvum lacks the novo dNTP biosynthesis and relies on salvage for dNTP biosynthesis. Thus, *Up*TK is needed to provide dTTP for DNA repair and replication. Previous studies[11,17,18] also demonstrated that *Up*TK is a promising drug target for antibiotic development. TK sequence alignment from various microorganisms and structural alignment of hTK1 and *Up*TK revealed that small differences exist between the enzymes, especially in the P-β hairpin and lasso loop. Here hTK1 and *Vv*-TK with shorter lasso loop appeared to form one subgroup, while the bacterial TKs form another. The *Up*TK lasso loop was the only TK in this alignment containing a Cys183 with unknown functional role. Gerland et al.[40] synthesised dThd nucleoside analogues harbouring 3́-disulfide substitutions, which were shown to be activated by hTK1 and they had promising anti-HIV activity. These types of analogs could be a starting point for targeting the Cys183 in *Up*TK.

Substitutions in the 3́ of the sugar and the 3 and 5 position of base could increase the selectivity for bacterial kinases.[17] 3′-AZT is well tolerated by TK1 and served as a start point for 3́ triazole analogs synthesised and tested here.

Both hTK1 and *Up*TK were able to accept many 3́-analogs. Compounds **10** and **13** exhibit similar properties as substrate or inhib-

itors, but compound **13** was found to be the best substrate with hTK1 and the next best with *Up*TK. In the latter case compound **6** was the most efficient substrate. The other tested analogs achieved 3–10-fold higher activities with *Up*TK than with hTK1. The IC_{50}-values for these analogues revealed that hTK1 was usually more inhibited than *Up*TK (Table 2). Thus, the capacity to serve as acceptor was not correlated to the inhibitory effect and this fact has been observed previously.[17] However, none of the analogs were very potent inhibitors but compounds **6, 9, 12** and **13** exhibited among the best kinetic results and were subjected to antibacterial activity tests. All synthesized analogs have been tested for their inhibitory activity on *Up* growth as well as on uninfected phytohemagglutinin-stimulated primary human peripheral blood mononuclear (PBM), a T-lymphoblastoid cell line (CEM), or African green monkey kidney (Vero) cells.[38] None of these analogs displayed toxic effects neither inhibition of *Up* growth at the concentrations tested.

Compound **13** was modelled in the active site of *Up*TK and hTK1 and our analysis suggested that the 3́ substitutions of **1**–**13** may be positioned in two different conformations; conformation A and B. In conformation A, the plane of the triazole-phenyl rings was positioned between the hydrophobic part of lasso loop Gly182 and P-β hairpin Arg53. The terminal part of the phenol with the hydrophilic fluorine atom was probably exposed to solvent. The absence of specific amino acid interactions apparently results in similar K_m-values as seen with compounds **6**, **9**, **12** and **13** (Table S1).

Compound **13** was also modelled into the active site of hTK1; here in conformation B, the triazole-phenyl-fluorine stretches from the lasso loop through the P-β hairpin. In this case, there are two additional serines 63–64, which provide potential hydrogen donor interactions with the fluorine atom of **13**. The Tyr61 seems to be responsible for making this interaction possible; because it is extending the hTK1 hairpin enough for the triazole-phenyl moiety to avoid a clash with Arg60 (Fig. 5B and S4B). This may explain its apparent high affinity for hTK1 and in the absence of this fluorine atom; the K_m-values were 3–4-fold higher. The extra tyrosine is not observed in *Up*TK and the Arg53 may therefore block the triazole-phenyl moiety interactions with serine 54 (Fig. S4A), which explains that the most likely conformation in *Up*TK is A. In the case of hTK1, the 3́ substitution in conformation A may sterically clash against the Arg60 side chain (Fig. S4B) explaining that the most likely conformation in hTK1 is B.

Modelled compound **6** revealed additional amino acid differences between *Up*TK (Val179 and Pro48) and hTK1 (Glu173 and Tyr55), located in either the lasso loop or P-β hairpin (Fig. 5A and D and S5), possibly explaining why compound **6** is a better substrate for *Up*TK than hTK1.

Thus, each enzyme most likely has a preference for one of two substrate analog conformations and the active site of *Up*TK seems to be more flexible than that of hTK1. This fact may be further exploited in the design of more selective inhibitors that may block DNA precursor synthesis or in substrates that would be selectively activated and incorporated in bacterial cells.

4. Conclusion

An efficient and rapid procedure to synthesize new 3′-α-[1,2,3]triazol-3′-deoxythymidine analogs is presented and their biological testing involved kinetic, structural and modelling analyses with the key activation enzyme TK1, of human and bacterial origin. The results as well as those of others[41] revealed the importance of detailed knowledge of the structure–activity relationships in the TK1 enzyme family, especially in the absence of determined substrate–enzyme complex structures. An important difference in structure and function between the human and bacterial TK1 enzymes, related to sequence diversity in the active sites, was found. The minimal activity with hTK1 may be one explanation for the lack of biological activity observed previously with this type of analogues.[28] However, when a 3́-triazole dThd triphosphate was synthesized it could inhibit the HIV-RT activity in vitro.[28a] Information presented here may help in the design of new triazole compounds of medical interest in anti-*Ureaplasma* and other anti-microbial therapies with minimal effects on host cell proliferation.

5. Experimental section

5.1. Chemistry section

For the synthesis of 3′-thymidine derivatives, commercially available chemicals were reagent grade and used as received. The starting material for the triazoles was AZT, which was prepared as described previously.[42] The microwave was a Biotage AB Initiator EXP EU with a maximum power of 300 W. The vials used in the microwave were Emrys™ process vials 0.5–2 mL. The reactions were monitored by thin-layer chromatography (TLC) analysis using silica gel plates (kieselgel 60 F_{254}, E. Merck). Silica gel (Merck Kieselgel 60, 15–40 μm) was used for flash chromatography. Compounds were visualized by UV irradiation and by spraying with 2.5% phosphomolybdic acid in 95% EtOH, followed by charring at 150 °C. The ^1H and ^{13}C NMR spectra were recorded on a Brucker AVANCE DPX 250 Fourier transform spectrometer at 400 MHz for ^1H and 100 MHz for ^{13}C, respectively, using tetramethylsilane as the internal standard, unless otherwise stated. Chemical shifts are given in ppm and signals are reported as s (singlet), d (doublet), t (triplet), q (quartet), and m (multiplet). High Resolution Mass spectra were performed by the Mass Spectrometry Center of Emory University (Atlanta, USA) and Blaise Pascal University (Aubière, France). The purity was determined by semi-preparative HPLC (Hypersil 100; C-18; 5 μm); with an appropriate gradient of acetonitrile/H_2O; purity of key target compounds was >95%.

5.1.1. 3′-(4-Hydroxymethyl-1,2,3-triazol-1-yl)-3′-deoxythymidine (1)

3′-Azido-3′-deoxythymidine (50 mg, 0.19 mmol) was dissolved in mix solvent *tert*-BuOH/H_2O 1/1 (2 mL), Cu(0) (0.8 equiv), $CuSO_4$ (1 M) 38 μL and propargyl alcohol (0.2 mmol). The mixture was stirred under microwave irradiation at 125 °C during 10 min. The solvent was removed under reduced pressure and the crude residue purified using flash chromatography with an elution gradient AcOEt to AcOEt/MeOH. Yield: 80% (49 mg) as white solid. CAS registration: 127479-69-0. ^1H NMR (CD_3OD) δ 1.91 (*s*, 3H, CH_3), 2.75 (m, 1H, H-2′b), 2.91 (m, 1H, H-2′a), 3.77 (dd, 1H, *J* = 2.8, 12.3 Hz, H-5′b), 3.91 (dd, 1H, *J* = 2.8, 12.3 Hz, H-5′a), 4.37 (dt, 1H, *J* = 2.8, 5.4 Hz, H-4′), 4.69 (s, 2H, CH_2), 5.44 (dt, 1H, *J* = 5.4, 8.2 Hz H-3′), 6.48 (t, *J* = 6.3 Hz, 1H, H-1′), 7.91 (s, 1H, H-6), 8.07 (s, 1H, C*H*=); ^{13}C NMR (CD_3OD) 12.5(*C*H_3), 39.1(C-2′), 61.0(*C*H_2–OH), 62.1(C-3′), 62.8(C-5′), 86.4(C-4′), 86.7(C-1′), 100.1(C-5), 111.7(C=), 127.3(C=), 138.3(C-6), 152.4(C-2), 166.4(C-4). HRMS (M^++H) 324.13000, calcd for $C_{13}H_{18}N_5O_5$ 324.13025.

5.1.2. 3′-(4-(2-Hydroxy-ethyl)-1,2,3-triazol-1-yl)-3′-deoxythymidine (2)

Compound **2** was prepared as described for **1** starting from AZT (50 mg, 0.19 mmol) and 3-but-1-yn-1-ol (0.2 mmol) under microwave during 10 min, yield: 82% (52 mg) as white solid. mp = 218–220 °C, ^1H NMR (CD_3OD) : 1.91(d, 3H, *J* = 1.0 Hz, CH_3), 2.75(dd, 1H, *J* = 6.4, 8.8, 14.8 Hz, H-2′b), 2.88–2.94 (m, 3H, H-2′a and CH_2), 3.76 (dd, 1H, *J* = 2.9, 12.3 Hz, H-5′b), 3.81 (m, 2H, C*H*$_2$OH), 3.91 (dd, 1H, *J* = 2.9, 12.3 Hz, H-5′a), 4.36 (dt, 1H, *J* = 2.9, 5.6 Hz, H-4′), 5.40(dt, 1H, *J* = 5.6, 8.3 Hz, H-3′), 6.48(t, 1H, *J* = 6.3 Hz, H-1′),

7.91(d, 1H, J = 1.0 Hz, H-6), 7.94 (s, 1H, C*H*=); ^{13}C NMR (CD_3OD) : 12.5(*C*H$_3$), 29.9(*C*H2), 39.0(C-2′), 60.9(C-3′), 62.0(*C*H$_2$–OH), 62.1(C-5′), 86.4(C-4′), 86.7(C-1′), 111.7(C-5), 123.8(*C*H=), 138.3(C-6), 152.3(C-2), 166.4(C-4). HRMS (M^++H) 338.14548, calcd for $C_{14}H_{20}N_5O_5$ 338.14590. Purity HPLC 99.2%, t_R = 3.7 min acetonitrile/H_2O (20:80, vol/vol).

5.1.3. 3′-(4-Methoxymethyl-1,2,3-triazol-1-yl)-3′-deoxythymidine (3)

Compound **3** was prepared as described for **1** starting from AZT (50 mg, 0.19 mmol) and methyl propargyl ether (0.2 mmol) under microwave during 10 min, yield: 90% (57 mg) as white solid. mp: 208–210 °C. ^{1}H NMR (CD_3OD) 1.90 (d, 3H, J = 1.2 Hz, T-CH$_3$), 2.75 (ddd, 1H, J = 6.0, 8.4, 14.2 Hz, H-2′b), 2.91 (ddd, 1H, J = 5.6, 6.8, 14.2 Hz,, H-2′a), 3.38 (s, 3H, OCH$_3$), 3.77 (dd, 1H, J = 3.0, 12.3 Hz, H-5′b), 3.91 (dd, 1H, J = 3.0, 12.3 Hz, H-5′a), 4.36 (dt, 1H, J = 3.0, 5.6 Hz, H-4′), 4.54 (s, 2H, –CH$_2$O), 5.44 (dt, 1H, J = 5.2, 8.4 Hz, H-3′), 6.48 (t, 1H, J = 6.4 Hz, H-1′), 7.91 (d, 1H, J = 1.2 Hz, H-6), 8.11 (s, 1H, C*H*=). ^{13}C NMR (CD_3OD) 12.5 (CH$_3$), 39.0 (C-2′), 58.2 (*C*H$_2$–O), 61.1 (C-3′), 62.1 (C-5′), 66.3 (O–CH$_3$), 86.4 (C-4′), 86.7 (C-1′), 111.7 (C-5), 124.8 (C=), 138.3 (C-6), 152.3 (C-2), 166.3 (C-4). HRMS (M^++H) 338.14551, calcd for $C_{14}H_{20}N_5O_5$ 338.14590. Purity HPLC 99.6%, t_R = 4.7 min acetonitrile/H_2O (20:80, vol/vol).

5.1.4. 3′-(4-Methylpropionate-1,2,3-triazole-1-yl)-3′-deoxythymidine (4)

Compound **4** was prepared as described for **1** starting from AZT (50 mg, 0.19 mmol) and propargyl acetate (0.2 mmol) under microwave during 2 min. Yield: 81% (56 mg) as white solid. mp: 128–130 °C. ^{1}H NMR (CD_3OD) 1.90 (s, 3H, CH$_3$), 2.05 (s, 3H, OAc), 2.70 (ddd, 1H, J = 6.4, 8.8, 14.4 Hz,, H-2′b), 2.90 (ddd, 1H, J = 5.2, 6.8, 14.4 Hz, H-2'a), 3.77 (dd, 1H, J = 2.8, 12.3 Hz, H-5′b), 3.91 (dd, 1H, J = 2.8, 12.3 Hz, H-5′a), 4.36 (dt, 1H, J = 2.8, 5.6 Hz, H-4′), 5.18 (s, 2H, CH$_2$), 5.43 (dt, 1H, J = 5.6, 8.5 Hz, H-3′), 6.48 (t, 1H J = 6.3 Hz, H-1′), 7.90 (s, 1H, H-6), 8.15 (s, 1H, C*H*=); ^{13}C NMR (CD_3OD) 12.5 (CH$_3$), 20.6 (CO*C*H$_3$), 39.0 (C-2′), 58.2 (*C*H$_2$-OAc), 61.1 (C-3′), 62.1 (C-5′), 86.3 (C-4′), 86.7 (C-1′), 111.7 (C-5), 125.6 (C=), 138.2 (C-6), 140.7 (C=), 152.3 (C-2), 166.3 (C-4), 172.3 (C=O). HRMS (M^++H) 366.14056, calcd for $C_{15}H_{20}N_5O_6$ 366.14081. Purity HPLC 99.9%, t_R = 11.5 min acetonitrile/H_2O (15:85, vol/vol).

5.1.5. 3′-(4-(3-Chloro-propyl)-1,2,3-triazol-1-yl)-3′-deoxythymidine (5)

Compound **5** was prepared as described for **1** starting from AZT (50 mg, 0.19 mmol) and 5-chloropentyne (0.2 mmol) under microwave during 30 min, yield: 78% (55 mg) as white solid. mp = 203–205 °C. ^{1}H NMR (CD_3OD) δ 1.91 (d, 3H, J = 1.0 Hz, T-CH$_3$), 2.13 (m, 2H, CH$_2$b), 2.71 (m, 1H, H-2′b), 2.88 (t, 2H, J = 7.2 Hz, CH$_{2a}$), 2.90 (m, 1H, H-2′a), 3.61 (t, 2H, J = 6.3 Hz, CH$_{2c}$), 3.76 (dd, 1H, J = 3.0, 12.3 Hz, H-5′b), 3.89 (dd, 1H, J = 3.0, 12.3 Hz, H-5′a), 4.35 (dt, 1H, J = 3.0, 5.8 Hz, H-4′), 5.39 (dt, 1H, J = 5.5, 8.5 Hz, H-3′), 6.47 (t, 1H, J = 6.4 Hz, H-1′), 7.90 (br d, 1H, J = 1.0 Hz, H-6), 7.92 (s, 1H, C*H*=); ^{13}C NMR (CD_3OD) 12.5(T-CH$_3$), 23.5(*C*H$_2$), 33.24(*C*H$_2$), 39.0(C-2′), 44.8(CH$_2$), 60.9(C-3′), 62.1(C-5′), 86.4(C-4′), 86.7(C-1′), 111.6(C-5), 123.2(C=), 138.3(C-6), 148.0(C=), 152.3(C-2), 166.4(C-4). HRMS (M^++H) 370.12758, calcd for $C_{15}H_{21}{}^{34}Cl_1N_5O_4$ 370.12766. Purity HPLC 99.0%, t_R = 18.45 min; acetonitrile/H_2O (20:80, vol/vol).

5.1.6. 3′-(4-Propyl-1,2,3-triazol-1-yl)-3′-deoxythymidine (6)

Compound **6** was prepared as described for **1** starting from AZT (50 mg, 0.19 mmol) and 1-pentyne (0.2 mmol) under microwave during 120 min, yield: 85% (54 mg) as white solid. mp: 210–212 °C. ^{1}H NMR (CD_3OD) 0.97 (t, 3H, J = 7.3 Hz, CH$_{3c}$), 1.69 (six, 2H, J = 7.3 Hz, CH$_{2b}$), 1.91 (d, 3H, J = 1.0 Hz, T-CH$_3$), 2.68 (t, 2H, J = 7.2 Hz, CH$_{2a}$), 2.71 (m, 1H, H-2′b), 2.90 (m, 1H, H-2′a), 3.76 (dd, 1H, J = 3.1, 12.3 Hz, H-5′b), 3.89 (dd, 1H, J = 3.1, 12.3 Hz, H-5′a), 4.35 (dt, 1H, J = 3.0, 5.8 Hz, H-4′), 5.39 (dt, 1H, J = 5.8, 8.5 Hz, H-3′), 6.47 (t, 1H, J = 6.4 Hz, H-1′), 7.87 (s, 1H, C*H*=), 7.91 (d, 1H, J = 1.0 Hz, H-6); NMR ^{13}C (CD_3OD) 12.5(T-CH$_3$), 13.9(CH$_3$), 23.7(*C*H$_2$), 28.9(*C*H$_2$), 39.0(C-2′), 60.8(C-3′), 62.1(C-5′), 86.4(C-4′), 86.7(C-1′), 111.7 (C-5), 122.8(*C*=), 138.3(C-6), 149.6(*C*=), 152.3(C-2), 166.4(C-4). Purity HPLC 95.1%, t_R = 32.4 min acetonitrile/H_2O (15:85, vol/vol).

5.1.7. 3′-(4-*tert*-Butyl-1,2,3-triazol-1-yl)-3′-deoxythymidine (7)

AZT (100 mg, 0.374 mmol) and 3,3-dimethyl-1-butyne (0.412 mmol) were suspended in a 1:1 mixture of water and *tert*-butanol (4 mL). Then, sodium ascorbate (0.1 equiv) and $CuSO_4$ (0.01 equiv) were added and the reaction mixture was stirred until the complete disappear of starting material. The solvent was removed under reduced pressure and the crude residue purified using flash chromatography with an elution gradient AcOEt/EtOH to AcOEt/MeOH. Yield: 82% (107 mg) as white solid. mp: 138–140 °C. ^{1}H NMR ($CDCl_3$) δ 1.35 (s, 9H, CH$_{3\ tert\text{-}but}$), 1.93 (s, 3H, T-CH$_3$), 2.90–2.95 (m, 2H, H-2′), 3.79 (dd, 1H, J = 2.4, 12.4 Hz, H-5′b), 4.02 (dd, 1H, J = 2.2, 12.4 Hz, H-5′a), 4.43 (dt, 1H, J = 2.2, 4.8 Hz, H-4′), 5.39 (dt, 1H, J = 5.7, 8.2 Hz, H-3′), 6.22 (t, 1H, J = 6.6 Hz, H-1′), 7.36 (s, 1H, C*H*=), 7.43 (d, 1H, J = 1.0 Hz, H-6); 8.92 (s, 1H, N*H*), NMR ^{13}C ($CDCl_3$) : 12.4(T-CH$_3$), 30.3(3 CH$_3$), 30.8(*C*–CH$_3$), 37.5(C-2′), 60.0(C-3′), 61.7(C-5′), 85.3(C-4′), 89.0 (C-1′), 111.3 (C-5), 118.5(*C*=), 137.9(C-6), 150.3(C-2), 158.1 (*C*=), 163.5(C-4) Purity HPLC 99.4%, t_R = 22.6 min; acetonitrile/H_2O (20:80, vol/vol).

5.1.8. 3′-(4-Pentyl-1,2,3-triazol-1-yl)-3′-deoxythymidine (8)

Compound **7** was prepared as described for **1** starting from AZT (50 mg, 0.19 mmol) and 1-heptyne (0.2 mmol) under microwave during 100 min, yield: 91% (63 mg) as white solid. Mp = 132–134 °C. ^{1}H NMR (CD_3OD) δ: 0.91 (t, 3H, J = 7.4 Hz, CH$_3$e), 1.37 (m, 4H, CH$_{2b}$ et CH$_{2c}$), 1.68 (t, 2H, J = 7.2 Hz, CH$_{2a}$), 1.91 (s, 3H, T-CH$_3$), 2.67–2.78 (m, 3H, H-2′b et CH$_{2d}$), 2.88 (m, 1H, H-2′a), 3.77 (dd, 1H, J = 3.1, 12.3 Hz, H-5′b), 3.91 (dd, 1H, J = 3.1, 12.3 Hz, H-5′a), 4.35 (dt, 1H, J = 3.0, 5.6 Hz, H-4′), 5.39 (dt, 1H, J = 5.6, 8.5 Hz, H-3′), 6.48 (t, 1H, J = 6.3 Hz, H-1′), 7.89 (s, 1H, H-6), 7.91 (s, 1H, C*H*=); ^{13}C NMR (CD_3OD) 12.5(*C*H$_3$), 14.3(*C*H$_{3e}$), 23.4, 26.3, 30.2, 32.5(4*C*H$_2$), 39.0(C-2′), 60.8(C-3′), 62.1(C-5′), 86.4(C-4′), 86.7(C-1′), 111.7(C-5), 122.8(C=), 138.3(C-6), 149.5(C=), 152.3(C-2), 166.4(C-4). HRMS (M^++H) 364.19748, calcd for $C_{17}H_{26}N_5O_4$ 364.19793. Purity HPLC 95.2%, t_R = 16.65 min acetonitrile/H_2O (30:70, vol/vol).

5.1.9. 3′-(4-Phenyl-1,2,3-triazol-1-yl)-3′-deoxythymidine (9)

Compound **9** was prepared as described for **1** starting from AZT (50 mg, 0.19 mmol) and phenylacetylene (0.2 mmol), under microwave during 20 min, yield: 84% (59 mg) as white solid. CAS registration: 127728-29-4. ^{1}H NMR (CD_3OD) 1.91(s, 3H, T-CH$_3$), 2.78 (m, 1H, H-2′b), 2.97 (m, 1H, H-2′a), 3.82 (dd, 1H, J = 2.9, 12.2 Hz, H-5′b), 3.94 (dd, J = 2.9, 12.2 Hz, 1H, H-5′a), 4.43 (dt, 1H, J = 2.9, 5.6 Hz, H-4′), 5.48 (dt, 1H, J = 5.6, 8.5 Hz, H-3′), 6.52 (t, J = 6.6 Hz, 1H, H-1′), 7.34–7.46 (m, 3H, H$_{arom}$), 7.83 (d, 2H, J = 7.8 Hz, H$_{arom}$), 7.93 (s, 1H, H-6), 8.47(s, 1H, C*H*=); ^{13}C NMR (CD_3OD) 12.5(*C*H$_3$), 39.1(C-2′), 61.1(C-3′), 62.2(C-5′), 86.4(C-4′), 86.7(C-1′), 111.7(C-5), 121.9(C=), 126.7, 129.5, 130.0(6 C$_{arom}$), 134.1(C=), 138.3(C-6), 152.3(C-2), 166.3(C-4). HRMS (M^++H) 370.15055, calcd for $C_{18}H_{20}N_5O_4$ 370.15098. Purity HPLC 98.9%, t_R = 10.0 min acetonitrile/H_2O (30:70, vol/vol).

5.1.10. 3′-(4-Benzyl-1,2,3-triazol-1-yl)-3′-deoxythymidine (10)

AZT (100 mg, 0.374 mmol) and 3-phenyl-1-propyne (0.412 mmol) were suspended in a 1:1 mixture of water and *tert*-butanol (4 mL). Then sodium ascorbate (0.1 equiv) and $CuSO_4$

(0.01 equiv) were added and the reaction mixture was stirred until the complete disappear of starting material. The solvent was removed under reduced pressure and the crude residue purified using flash chromatography with an elution gradient AcOEt/EtOH to AcOEt/MeOH. Yield: 84% (120 mg) as white solid: mp = 120–122 °C. ^{1}H NMR (CD_3OD) 1.89 (s, 3H, T-CH_3), 2.69 (ddd, 1H, J = 6.4, 8.6, 14.2 Hz, H2′b), 2.87 (dt, 1H, J = 6.0, 14.2 Hz, H2′a), 3.73 (dd, 1H, J = 3.2, 12.4 Hz, H5′b), 3.88 (dd, J = 3.2, 12.4 Hz, 1H, H5′a), 4.05 (s, 2H, CH_2–Ph), 4.33 (dt, 1H, J = 3.2, 6.0 Hz, H4′), 5.36 (dt, 1H, J = 6.0, 8.4 Hz, H3′), 6.45 (t, 1H, J = 6.4 Hz, H1′), 7.17–7.30 (m, 5H, H_{arom}), 7.83(s, 1H, CH=); 7.88 (s, 1H, H6). ^{13}C NMR (CD_3OD) 12.5(CH_3), 32.6(CH_2), 39.0(C-2′), 60.9(C-3′), 62.1(C-5′), 86.4(C-4′), 86.7(C-1′), 111.7(C-5), 123.5(C=), 127.6(2 C_{arom}), 126.5, 129.6, 129.7 (3 C_{arom}), 138.3(C-6), 140.3(C_{arom}), 148.8(C=), 152.3(C-2), 166.4(C-4). Purity HPLC 95.9%, t_R = 10.0 min acetonitrile/H_2O (30:70, vol/vol).

5.1.11. 3′-(4-(2-Phenyl-ethyl)-1,2,3-triazole-1-yl)-2′-deoxythymidine (11)

AZT (100 mg, 0.374 mmol) and 4-phenyl-1-butyne (0.412 mmol) were suspended in a 1:1 mixture of water and *tert*-butanol (4 mL). Then sodium ascorbate (0.1 equiv) and $CuSO_4$ (0.01 equiv) were added and the reaction mixture was stirred until the complete disappear of starting materiel. The solvent was removed under reduced pressure and the crude residue purified using flash chromatography with an elution gradient AcOEt/EtOH to AcOEt/MeOH. Yield: 86% (127 mg) as white solid mp = 150–152 °C. ^{1}H NMR (CD_3OD) δ 1.90 (s, 3H, T-CH_3), 2.69 (ddd, 1H, J = 6.0, 8.4, 14.4 Hz, H2′b), 2.85 (m, 1H, H2′a), 2.95–3.04 (m, 4H, 2 CH_2), 3.71 (dd, 1H, J = 3.0, 12.0 Hz, H5′b), 3.87 (dd, J = 3.0, 12.0 Hz, 1H, H5′a), 4.29 (dt, 1H, J = 3.0, 6.0 Hz, H4′), 5.34 (dt, 1H, J = 6.0, 8.8 Hz, H3′), 6.44 (t, 1H, J = 6.4 Hz, H1′), 7.15 (m, 3H, H_{arom}), 7.24 (m, 2H, H_{arom}), 7.72(s, 1H, CH=); 7.89 (s, 1H, H6). ^{13}C NMR (CD_3OD) 12.5(CH_3), 28.4(CH_2), 36.5(CH_2), 39.0(C-2′), 60.7(C-3′), 62.0(C-5′), 86.4(C-4′), 86.7(C-1′), 111.7(C-5), 123.2(C=), 127.6(2 C_{arom}), 126.4, 129.5, 129.6 (3 C_{arom}), 138.3(C-6), 142.3(C_{arom}), 148.6(C=), 152.3(C-2), 166.4(C-4). Purity HPLC 99.6%, t_R = 14.6 min acetonitrile/H_2O (30:70, vol/vol).

5.1.12. 3′-(4-(2-Pyridine)-1,2,3-triazole-1-yl)-2′-deoxythymidine (12)

Compound **12** was prepared as described for **1** starting from AZT (50 mg, 0.19 mmol) and 2-ethynylpyridine (0.2 mmol), under microwave during 10 min, yield: 86% (60 mg) as white solid. CAS registration: 127479-76-9. ^{1}H NMR (CD_3OD) δ 1.91 (s, 3H, T-CH_3), 2.79 (m, 1H, H-2′b), 2.97 (m, 1H, H-2′a), 3.82 (dd, 1H, J = 2.9, 12.2 Hz, H-5′b), 3.94 (dd, J = 2.9, 12.2 Hz, 1H, H-5′a), 4.41 (dt, 1H, J = 2.9, 5.6 Hz, H-4′), 5.52 (dt, 1H, J = 5.6, 8.5 Hz, H-3′), 6.53 (t, J = 6.6 Hz, 1H, H-1′), 7.36 (m, 1H, H_{pyr}), 7.91 (m, 2H, H_{pyr}), 8.10 (d, 1H, J = 8.1 Hz, H_{pyr}), 8.57 (br s, 2H, CH= and H-6). ^{13}C NMR (CD_3OD) : 12.5(CH_3), 39.1(C-2′), 61.3(C-3′), 62.1(C-5′), 86.4(C-4′), 86.7(C-1′), 111.7(C-5), 121.9(C=), 120.7, 124.0, 136.2, 148.8, 158.3 (C_{arom}), 138.3(C-6), 150.9(C-2), 166.4(C-4). HRMS (M^++H) 371.14584, calcd for $C_{17}H_{19}N_6O_4$ 371.14678. Purity HPLC 99.2%, t_R = 5.53 min acetonitrile/H_2O (30:70, vol/vol).

5.1.13. 3′-(4-(4-Fluorophenyl)-1,2,3-triazole-1-yl)-2′-deoxythymidine (13)

Compound **13** was prepared as described for **1** starting from AZT (50 mg, 0.19 mmol) and 1-ethynyl-4-fluorobenzene (0.2 mmol), under microwave during 20 min, yield: 96% (71 mg) as white solid. CAS registration: 127479-75-8. ^{1}H NMR (CD_3OD) δ 1.88 (d, 3H, J = 1.0 Hz, T-CH_3), 2.78 (ddd, 1H, J = 6.0, 8.4, 14.2 Hz, H2′b), 2.94 (ddd, 1H, J = 5.6, 6.8, 14.2 Hz, H2′a), 3.82 (dd, 1H, J = 2.9, 12.2 Hz, H-5′b), 3.93 (dd, J = 2.9, 12.2 Hz, 1H, H-5′a), 4.44 (dt, 1H, J = 2.9, 5.3 Hz, H-4′), 5.46 (dt, 1H, J = 5.3, 8.4 Hz, H-3′), 6.50 (t, J = 6.2 Hz, 1H, H-1′), 7.14 (m, 2H, H_{arom}), 7.83 (m, 2H, H_{arom}), 7.90 (d, 1H, J = 1.0 Hz, H-6), 8.42 (s, 1H, CH=); ^{13}C NMR (CD_3OD) 12.5(CH_3), 39.1(C-2′), 61.1(C-3′), 62.2(C-5′), 86.4(C-4′), 86.7(C-1′), 111.7(C-5), 116.8(d, J = 21.3 Hz, 2 C_{arom}), 121.8(C=), 123.9(C_{arom}), 128.7(d, J = 7.3 Hz, 2 C_{arom}), 138.3(C-6), 148.2, (C=), 164.2(d, J = 234.6 Hz, C_{arom}), 152.3(C-2), 166.2(C-4), HRMS (M^++H) 388.14105, calcd for $C_{18}H_{19}FN_5O_4$ 388.14211. Purity HPLC 98.48%, t_R = 14.13 min acetonitrile/H_2O (30:70, vol/vol).

5.2. Biology section

The none-radioactive-labelled substances dThd/dUrd were from (Sigma Aldrich) and radiolabeled substance [γ-^{32}P]-ATP (3000 Ci mmol^{-1}) was from Perkin–Elmer. All compounds **1–13** (Fig. 2) were diluted in DMSO and the nucleosides dThd and AZT in sterile H_2O.

5.3. Enzyme relative activity, kinetics and IC_{50} determination

Recombinant *Up*-TK and hTK1 enzymes were expressed and purified as described previously.[11,18] Phosphate transfer assay with 100 M [γ-^{32}P] ATP was used to determine TK activities as previously described with some modifications.[11,16,17] In short, 100 M of dThd and dThd-analogues with 5 ng *Up*-TK or 10 ng hTK1 were used. The mixtures were incubated for 15 min for *Up*TK and 20 min for hTK1 at 37 °C and heat-inactivated at 95 °C for 2 min. The relative activity was expressed using the activity with dThd as 100%. The kinetic parameters were determined with different substrate concentrations for example, dThd 2–20 M for 0.5 ng *Up*TK and 2–50 M for 1 ng hTK1. The standard reaction contain 10–500 M dThd-analogues with 10 ng *Up*TK or -hTK1, 50 mM Tris/HCl pH 7.6, 5 mM $MgCl_2$, 100 μM [γ-^{32}P]-ATP, 0.5 mg/ml BSA and 10 mM DTT. The final DMSO concentration did not exceed 5% in the reaction solution. The reactions were performed for 20 min at 37 °C and then heat-inactivated at 95 °C for 2 min. Two microlitres of the reaction solutions were spotted on PEI-TLC plates, which were developed in 33 mL dH_2O, 66 ml *iso*-butyric acid and 1 mL NH_4. Quantification was done by phosphoimaging analysis (Fujifilm Image Gauge, version 3.3). The enzyme kinetic parameters K_m, V_{max}, *and* V_{max}/K_m were calculated by using the Michaelis Menten equation with the SigmaPlot Enzyme Kinetic Module version 2.1 (SPSS Science, Chicago, IL). The mean and standard error of mean (SEM) for relative activity %, K_m and V_{max} values were calculated from three independent determinations.

The inhibitory concentration at 50% (IC_{50}) were determined by using DE-81 filter paper technique and the [^{3}H]-dThd assay. The standard reaction contained 2 mM $MgCl_2$, 5 mM ATP, fixed 1 M [^{3}H]-dThd, 5 mM DTT, 0,5 ng *Up*TK and 4 ng hTK1 to achieve similar and comparable activity. Nucleoside analog concentrations of 10–500 M (1–20 M for AZT) competing with 1 M [^{3}H]-dThd in total volume of 50 L were used. The reaction temperature was 25 °C for both enzymes in order to keep the total conversion of substrate to product below 25%. The filters with 10 L fractions of the reaction solutions were washed three times in 10 mM ammonium formate and once in water. The reaction products were eluted with 0.5 mL 0.1 M HCl/0.2 M KCl and radioactivity was determined by liquid scintillation counting (Beckman). Relative inhibition was set to 100% for dThd with no nucleoside analogs and IC_{50} was estimated by the Biofitdata tool (Change Bioscience) http://www.changbioscience.com/stat/ec50.html.

One unit of kinase activity was defined as the formation of 1 nmol deoxyribonucleoside 5′-monophosphate per milligram protein per minute.

5.4. Sequence and structure sources

TK sequences from human (P04183), gram positive sequences; *U. parvum* (Q9PPP5), *Bacillus antracis* (Q81JX0), and gram negative bacteria; *E. coli* (P23331), *Yersinia pestis* (Q8ZEJ1), *V. virus* (P68563) were downloaded from protein knowledgebase (http://www.uniprot.org/) and pasted in ClustalW2 (http://www.ebi.ac.uk/Tools/clustalw2/index.html) tool according to instructions with default settings. Monomers with crystal structures for; hTK1 1XBT (chain G) and *Up*TK 2UZ3 (chain B) were superimposed using the PyMOL graphic system (DeLano Scientific).

5.5. Computational studies of human TK1 and *Ureaplasma* TK

The structures of the B chain of *Up*TK (2UZ3) and chain A of hTK1 (1W4R) were saved in separate pdb-file. The hTK1 (1XBT) structure were not used for modelling because residues connected to serine 64 of the P-hairpin loop was disordered. The Mg^{2+} atom was absent in 1W4R, but the ion coordinates could be added to this structure by superimposing both structure (0.158 Å for 157 Cα atoms) with each other in PyMOL graphic system (DeLano Scientific). The analog structures in 2D format were created by the Marvin sketch program from the Marvin beans package (http://www.chemaxon.com/). They were also saved in Smile format and further converted to pdb format at 'Online SMILIES translator' (http://cactus.nci.nih.gov/services/translate/). Modelling of the best accepted triazole-nucleoside, substrate and inhibitor compound **13** was used for modelled by the Arguslab[43] program (www.arguslab.com). The binding site was defined from the coordinates of the ligand main chain bonds (dTTP) in the original PDB files of hTK1 (1W4R), respectively *Up*TK (2UZ3). The modelling settings were set to 'high' and 'flexible ligand docking.' The chosen conformations were then saved in pdb format and visualized with PyMOL.

Acknowledgments

This work was supported by grants from the Swedish Research Council for the Environment, Agricultural Sciences and Spatial Planning (FORMAS), and the Swedish Research Council to S.E. UMPC-Paris 6 and the Centre National de la Recherche Scientifique (Unité Propre de Recherche 3082 and Formation de Recherche en Evolution 2852), Agence Nationale de Recherche Grant ANR-05-BLAN-0368-02 (to L.A.A. and D.D.-B.). This work was also supported in part by NIH Grant 4R37-AI-025899, 5R37-AI-041980, 5P30-AI-50409 (CFAR), and by the Department of Veterans Affairs to R.F.S.

Supplementary data

Supplementary data associated with this article can be found, in the online version, at doi:10.1016/j.bmc.2010.03.023.

References and notes

1. Eriksson, S.; Munch-Petersen, B.; Johansson, K.; Eklund, H. *Cell. Mol. Life Sci.* **2002**, *59*, 1327.
2. Johansson, K.; Ramaswamy, S.; Ljungcrantz, C.; Knecht, W.; Piskur, J.; Munch-Petersen, B.; Eriksson, S.; Eklund, H. *Nat. Struct. Biol.* **2001**, *8*, 616.
3. Johansson, N. G.; Eriksson, S. *Acta Biochim. Pol.* **1996**, *43*, 143.
4. Sherley, J. L.; Kelly, T. J. *J. Biol. Chem.* **1988**, *263*, 8350.
5. Al-Madhoun, A. S.; Tjarks, W.; Eriksson, S. *Mini-Rev. Med. Chem.* **2004**, *4*, 341.
6. Hallek, M.; Wanders, L.; Strohmeyer, S.; Emmerich, B. *Ann. Hematol.* **1992**, *65*, 1.
7. Camerman, A.; Mastropaolo, D.; Camerman, N. *Proc. Natl. Acad. Sci. U.S.A.* **1987**, *84*, 8239.
8. Elwell, L. P.; Ferone, R.; Freeman, G. A.; Fyfe, J. A.; Hill, J. A.; Ray, P. H.; Richards, C. A.; Singer, S. C.; Knick, V. B.; Rideout, J. L., et al *Antimicrob. Agents Chemother.* **1987**, *31*, 274.
9. Wang, J.; Neuhard, J.; Eriksson, S. *Antimicrob. Agents Chemother.* **1998**, *42*, 2620.
10. Glass, J. I.; Lefkowitz, E. J.; Glass, J. S.; Heiner, C. R.; Chen, E. Y.; Cassell, G. H. *Nature* **2000**, *407*, 757.
11. Carnrot, C.; Wehelie, R.; Eriksson, S.; Bolske, G.; Wang, L. *Mol. Microbiol.* **2003**, *50*, 771.
12. Bizarro, C. V.; Schuck, D. C. *Gen. Mol. Biol.* **2007**, *30*, 190.
13. Pollack, J. D. *Trends Microbiol.* **2001**, *9*, 169.
14. Hudson, M. M.; Talbot, M. D. *Int. J. STD AIDS* **1997**, *8*, 546.
15. Waites, K. B.; Katz, B.; Schelonka, R. L. *Clin. Microbiol. Rev.* **2005**, *18*, 757.
16. Wang, L.; Westberg, J.; Bolske, G.; Eriksson, S. *Mol. Microbiol.* **2001**, *42*, 1065.
17. Kosinska, U.; Carnrot, C.; Eriksson, S.; Wang, L.; Eklund, H. *FEBS J.* **2005**, *272*, 6365.
18. Welin, M.; Kosinska, U.; Mikkelsen, N. E.; Carnrot, C.; Zhu, C.; Wang, L.; Eriksson, S.; Munch-Petersen, B.; Eklund, H. *Proc. Natl. Acad. Sci. U.S.A.* **2004**, *101*, 17970.
19. Birringer, M. S.; Claus, M. T.; Folkers, G.; Kloer, D. P.; Schulz, G. E.; Scapozza, L. *FEBS Lett.* **2005**, *579*, 1376.
20. Munch-Petersen, B.; Cloos, L.; Tyrsted, G.; Eriksson, S. *J. Biol. Chem.* **1991**, *266*, 9032.
21. Katritzky, A. R.; Zhang, Y.; Singh, S. K. *Heterocycles* **2003**, *60*, 1225. and references cited therein.
22. Chen, M. D.; Lu, S. J.; Yuag, G. P.; Yang, S. Y.; Du, X. L. *Heterocycl. Commun.* **2000**, *6*, 421.
23. Alvarez, R.; Velazquez, S.; San-Felix, A.; Aquaro, S.; De Clercq, E.; Perno, C. F.; Karlsson, A.; Balzarini, J.; Camarasa, M. *J. Med. Chem.* **1994**, *37*, 4185.
24. Manfredini, S.; Vicentini, C. B.; Manfrini, M.; Bianchi, N.; Rutigliano, C.; Mischiati, C.; Gambari, R. *Bioorg. Med. Chem.* **2000**, *8*, 2343.
25. Markov, V. I.; Polyakov, E. V. Organic Chemistry in Ukrine. **2005**, ARKIVOC (viii), 89.
26. Broggi, J.; Joubert, N.; Aucagne, V.; Zevaco, T.; Berteina-Raboin, S.; Nolan, S. P.; Agrofoglio, L. A. *Nucleosides Nucleotides Nucleic Acids* **2007**, *26*, 779.
27. Saito, Y.; Escuret, V.; Durantel, D.; Zoulim, F.; Schinazi, R. F.; Agrofoglio, L. A. *Bioorg. Med. Chem.* **2003**, *11*, 3633.
28. (a) Haebich, D.; Barth, W.; Roesner, M. *Heterocycles* **1989**, *29*, 2083; (b) Wigerinck, P.; Van Aerschot, A.; Claes, P.; Balzarini, J.; De Clercq, E.; Herdewijn, P. *J. Heterocycl. Chem.* **1989**, *26*, 1635; (c) Zhou, L.; Amer, A.; Korn, M.; Burda, R.; Balzarini, J.; De Clercq, E.; Kern, A. R.; Torrence, P. F. *Antiviral Chem. Chemother.* **2005**, *16*, 375.
29. (a) Kolb, H. C.; Sharpless, K. B. *Drug Discovery Today* **2003**, *8*, 1128; (b) Kolb, H. C.; Finn, M. G.; Sharpless, K. B. *Angew. Chem., Int. Ed.* **2001**, *40*, 2004.
30. Huisgen, R. *Angew. Chem., Int. Ed. Engl.* **1963**, *75*, 742.
31. (a) Piralli, T.; Pagliai, F.; Mercurio, C.; Boggio, R.; Canonico, P. L.; Sorba, G.; Tron, G. C.; Genazzani, A. *J. Comb. Chem.* **2008**, *10*, 624; For the use of azide- alkyne 1,3-dipolar huisgen cycloaddition in nucleoside chemistry see: (b) Amblard, F.; Cho, J. H.; Shinazi, R. F. *Chem. Rev.* **2009**, *109*, 4207.
32. Sandrini, M. P.; Clausen, A. R.; On, S. L.; Aarestrup, F. M.; Munch-Petersen, B.; Piskur, J. *J. Antimicrob. Chemother.* **2007**, *60*, 510.
33. Sandrini, M. P.; Shannon, O.; Clausen, A. R.; Bjorck, L.; Piskur, J. *Antimicrob. Agents Chemother.* **2007**, *51*, 2726.
34. For microwave-assisted syntheses of nucleosides see: Roy, V.; Pradère, U.; Agrofoglio, L. A. *Future Med. Chem.* **2010**, *2*, 177–192.
35. (a) Loupy, A. *Microwaves in Organic Synthesis;*; Wiley-VCH: Weinheim, Germany, 2002. and references cited therein; (b) Perez-Balderas, F.; Ortega-Munoz, M.; Morales-Sanfrutos, J.; Hernandez-Mateo, F.; Calvo-Flores, F. G.; Calvo-Asin, J. A.; Isac-Garcia, J.; Santoyo-Gonzalez, F. *Org. Lett.* **2003**, *5*, 1951; (c) Singh, P. N. D.; Muthukrishnan, S.; Murthy, R. S.; Klima, R. F.; Mandel, S. M.; Hawk, M.; Yarbrough, N.; Gudmundsdóttir, A. D. *Tetrahedron Lett.* **2003**, *44*, 9169; (d) Khanetskyy, B.; Dallinger, D.; Kappe, C. O. *J. Comb. Chem.* **2004**, *6*, 884; (e) Rijkers, D. T. S.; Esse, W. V.; Merks, R.; Brouwer, A. J.; Jacobs, H. J. F.; Pieters, R. J.; Liskamp, M. J. *Chem. Commun.* **2005**, *36*, 4581.
36. Appukkuttan, P.; Dehaen, W.; Fokin, V. V.; Van der Eycken, E. *Org. Lett.* **2004**, *6*, 4223.
37. Rostovtsev, V. V.; Green, L. G.; Fokin, V. V.; Sharpless, K. B. *Angew. Chem., Int. Ed.* **2002**, *41*, 2596.
38. Stuyver, L. J.; Lostia, S.; Adams, M.; Matthew, J.; Pai, B. S.; Grier, J.; Tharnish, P.; Choi, Y.; Chong, Y.; Choo, H.; Chu, C. K.; Otto, M. J.; Schinazi, R. F. *Antimicrob. Agents Chemother.* **2002**, *46*, 3854.
39. Sandrini, M. P.; Clausen, A. R.; Munch-Petersen, B.; Piskur, J. *Nucleosides Nucleotides Nucleic Acids* **2006**, *25*, 1153.
40. Gerland, B.; Desire, J.; Balzarini, J.; Decout, J. L. *Bioorg. Med. Chem.* **2008**, *16*, 6824.
41. Carnrot, C.; Wang, L.; Topalis, D.; Eriksson, S. *Protein Sci.* **2008**, *17*, 1486.
42. Czernecki, S.; Valéry, J. M. *Synthesis* **1991**, *3*, 239–240.
43. Joy, S.; Nair, P. S.; Hariharan, R.; Pillai, M. R. *In Silico Biol.* **2006**, *6*, 601–605.